

BIOMECHANICS OF BICYCLE PEDALLING

M. Jorge and M.L. Hull
Department of Mechanical Engineering
University of California
Davis, CA 95616

Abstract

Five pedalling conditions were investigated for three test subjects using a six load component pedal dynamometer. EMG electrodes simultaneously monitored the activity of eight leg muscles. Both pedal dynamometer and EMG data were digitized by a minicomputer. A five-bar linkage model of the leg-bicycle system was used to calculate the joint moments of the leg. Data analysis entailed generating plots of joint moments due to pedal load only and acceleration only. Total moments were produced by superimposing the two moment histories. The separate moment histories, together with the pedal forces and IEMG results, enable a detailed picture of the biomechanics of bicycle pedalling.

Introduction

Understanding the biomechanics of bicycle pedalling is important for several reasons. First, a thorough understanding of the mechanics involved in pedalling could lead to improvements in efficiency. Second, maximum benefits could be derived using stationary ergometers as a form of physical therapy if bicycling biomechanics is understood. Finally, thoroughly developing the science of bicycling would lead to techniques for improving performance in competition.

Information needed to understand the pedalling process includes identifying the leg muscles which participate, the pedal loads, and the kinematics of the leg segments. Studies of the leg muscles have been made. Houtz and Fischer [1] used a stationary exercise bicycle to study electromyograms of 14 surface muscles thought to be active while riding the device. Despires [2] used a bicycle which was ridden on a treadmill to study the effects of seat position and load on the activity of the surface muscles of the leg. In their book, Faria and Cavanagh [3] discuss the muscles and joints involved in cycling. Gregor, et al. [4] used a highly modified exercise ergometer with subjects wearing cleated shoes to establish a "normal" riding position for each of their subjects. Jorge and Hull [5] studied electromyograms of eight leg muscles of subjects riding a bicycle on rollers. Goto et al. [6] studied the relationship between the work load and frequency and the IEMG of leg muscles participating in pedalling and confirmed the relationship between IEMG and oxygen consumption.

Additional information needed to understand the whole pedalling process are pedal loading data and the kinematics of the leg. Literature in this area is sparse, however. Hoes et al. [7] measured crank and pedal forces of an ergometer. Gregor [8] used a racing bicycle with its front forks fixed and rear wheels on rollers. Tangential and normal pedal forces were obtained through a specially made pedal. Joint moments at the hip, knee, and ankle were then calculated using the kinematic and pedal data. Davis and Hull [9] used a six load component pedal dynamometer to measure the complete pedal loading. Nordeen-Snyder [10] used cinematography to extract kinematic data from the hip, knee, and ankle while subjects rode on rollers.

Previous work in the study of internal loads of the leg have been limited to the study of human gait. Winter and Robertson [11] conducted experiments on normal level gait to determine the synergistic patterns present in the forces causing joint moments. Zarrugh [12] computed ground reaction forces using kinematic data of the leg obtained from several walking speeds. Andrews [13] investigated the relationship between joint torques and *in vivo* muscular activity and concluded that the relationship cannot be determined by direct experimental measurements. Chao and Rim [14] presented a method based on inverse dynamics and optimization to determine the applied moments at the joints in human lower extremities during gait. Ghista et al. [15] presented an analysis of human gait and the resultant skeletal stresses of the lower limb. A finite element analysis was undertaken to determine the instantaneous stress in the lower limb. Seireg and Arvikar [16] developed a mathematical model of the lower extremity. A simplex algorithm was used to solve for muscle forces and joint reactions at static postures.

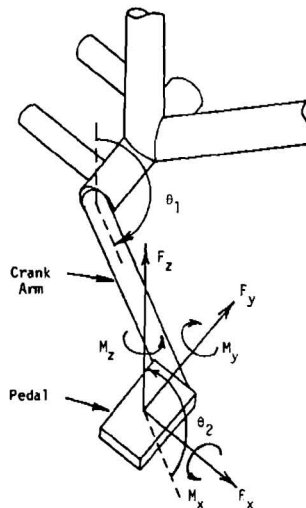


Fig. 1 Definition of Foot-Pedal Reactive Load Components, Crank-Arm Angle θ_1 , and Relative Pedal Angle θ_2

While these previous research efforts have provided valuable insight into the pedalling process, an interpretation of the results integrated with both kinematic data and pedal loading measurements has not been attempted. Further, a comprehensive analysis of internal leg loads has not been undertaken. Therefore, the objective of this paper is to present an integrated picture of bicycling biomechanics including muscle activity, pedal loads, and kinematics at different pedalling conditions.

Methods

The subjects in the experiment were three experienced male cyclists. Subject A's experience has come mainly from touring. Subject B is a recreational rider and is the least experienced of the three subjects. Subject C is a former racing cyclist who still participates in organized cycling events by the local bicycle club. Pertinent anthropomorphic data for the test subjects is given in Table 1.

TABLE 1. ANTHROPOMORPHIC DATA

SUBJECT	HEIGHT	WEIGHT	TROCHANTER LENGTH	EXPERIENCE
A	1.78 m	75.75 kg	0.89 m	tourist
B	1.75 m	74.75 kg	0.82 m	recreational rider
C	1.75 m	70.31 kg	0.90 m	former racer
SUBJECT	THIGH LENGTH	SHANK LENGTH	SPINDLE TO ANKLE DISTANCE	
A	.393 m	.433 m	.203 m	
B	.378 m	.381 m	.184 m	
C	.381 m	.431 m	.187 m	

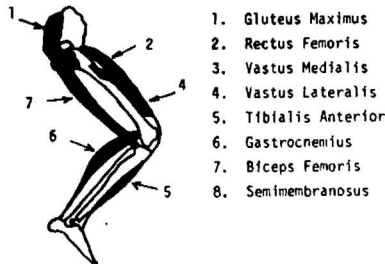
The bicycle that was used in the experiment is a Windsor Super Carrera which was ridden on rollers to simulate actual riding. Rollers simulate actual riding conditions because no lateral support is provided for the bicycle. Also, both wheels revolve and the rider must balance himself as in actual riding, thus giving the feeling of road conditions. Because tire pressure affects rolling friction, and therefore the work needed to turn the pedals, the tires were kept at a constant pressure during the experiment.

Despires [2] reported changes in muscle activity when the seat angle was changed. Accordingly, the seat that was used in the experiment was a Cool Gear patent no. 3807793 which was leveled to be horizontal. The seat height was adjusted to 100 percent of the trochanter length of each subject. This height is defined as the distance from the top of the seat to the surface of the pedal spindle, measured along the seat tube with the crank arm in the down position but parallel to the seat tube.

A six load component pedal dynamometer described by Hull and Davis [9] was used to collect the pedal force data. The pedal dynamometer measured reaction forces and moments about three axes. Figure 1 shows the coordinates used with the pedal dynamometer. Pedal and crank arm orientation was

determined by using 10 K ohm continuous potentiometers. Pedal load data was digitized and stored in an LSI-11/23 computer. Software written by Davis and Hull [17] was used to process the pedal data. Cadence was determined by using a PACER 2000 H, which is a bicycle computer capable of monitoring cadence, elapsed time, instantaneous speed, average speed, distance traveled, and heart rate.

Activity of the eight muscles listed in Fig. 2 was monitored using surface electrodes. To quantify relative muscle activity levels, the electrode signals were integrated over consecutive 75 ms intervals. Further details of the methods and materials relative to the EMG measurements may be found in Ref. [5].



Not Shown: Semimembranosus, Vastus Medialis

Fig. 2a. General Anatomy of the Leg

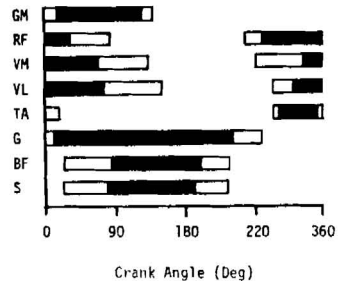


Fig. 2b. Muscle Timing Diagram

Data for the five pedalling conditions listed in Table 2 were recorded to explore the following hypotheses:

1. Joint moments are related to the pedal loading.
2. Joint moments required to accelerate the leg segments are strongly dependent on cadence and significant at higher cadences.
3. Joint moments are indicators of muscle activity levels.

TABLE 2
EMG EXPERIMENT

CASE	RPM	GEAR ¹	SHOES	SEAT HEIGHT ²
1	86	52 x 19	cleats	100 percent
3	63	52 x 15	cleats	100 percent
4	97	52 x 23	cleats	100 percent
5	80	52 x 23	cleats	100 percent
6	80	52 x 15	cleats	100 percent

¹ Gear ratio (number of teeth: chainwheel x cog)

² Percent of trochanter length

The human musculo-skeletal system can be modeled as a system of linkages [13] where the muscles and tendons around the joints are used to produce the moments necessary for joint motion. Hence, the leg-bicycle system was modeled as a five-bar linkage (see Fig. 3a) and kinematically analyzed to determine both the angular and absolute accelerations of the centers of mass of the four moving links (thigh, shank, foot, and crank). Solving the system of equations uniquely requires six input conditions: two angles, two angular velocities, and two angular accelerations. These conditions were determined from the measured pedal and crank angles. Inspection of the crank angle data vs time showed that the crank angular velocity could be assumed constant. Inspection of pedal angle data showed that the angle profile was represented well by a sinusoid. Accordingly, angular velocity and angular acceleration were obtained by first fitting a sinusoid to the pedal angle profile and then differentiating.

Joint moments were computed from the free-body diagram illustrated in Fig. 3b. Outside of the joint moments and joint reaction forces, the only other external loads are the foot-pedal normal F_z and tangential F_x force components. The force components were determined from the pedal dynamometer data. Note that the moment about the pedal spindle M_y is not included because this load component is negligible (see Hull and Davis [9]).

Model parameter values were obtained from several sources. Segment lengths were measured and are indicated in Table 2. Segment masses, CG locations, and moments of inertia were determined according to procedures recommended by Drillis [18].

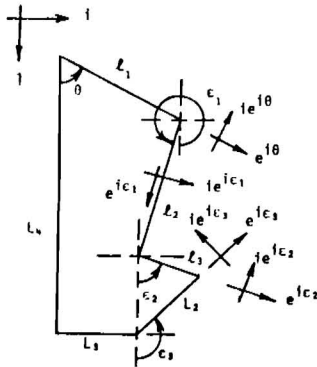


Fig. 3a Five-bar linkage model

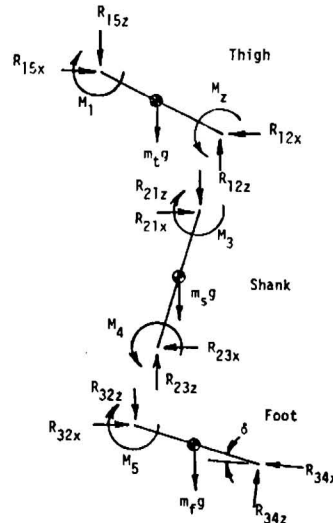


Fig. 3b Free-body diagram

Results

A. Reference Case

The ankle joint is the easiest to understand because of the low inertia of the foot. The two muscles which cross this joint are the gastrocnemius and the tibialis anterior. Examination of the region of muscle activity (see Fig. 2(b)) shows that the gastrocnemius is active between TDC and 280° . Between TDC and 130° the ankle moment due to pedal load increases (see Fig. 4(a)). This corresponds to the increase in the normal pedal force (see Fig. 4(b)). Note also that the ankle moment never goes below zero, which is consistent with the normal pedal force. The ankle moment due to acceleration (see Fig. 5(a)) is small compared with the moment due to the pedal force and hence can be considered negligible. Because of the similarity between the ankle moment and the normal pedal force, which corresponds with the region of gastroc activity, the gastrocnemius is active only to equilibrate the ankle joint moment. The maximum activity region, however, commences at about 20° and continues to about 250° . It is surprising that the maximum activity of the gastrocnemius extends beyond 200° . This is because the ankle moment due to pedal load is decreased significantly as is the normal pedal force. The gastroc activity beyond 200° is best explained by noting that the ankle is significantly extended during the backstroke. This extension would account for the sustained IEMG levels beyond 200° .

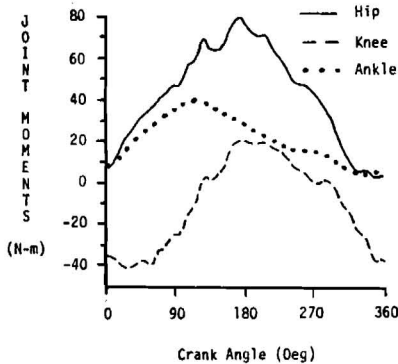


Fig. 4a Joint Moments Due to Pedal Forces (reference)

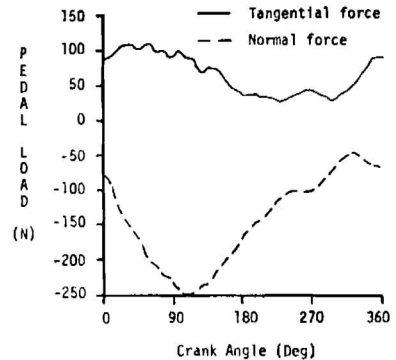


Fig. 4b Pedal Forces (reference)

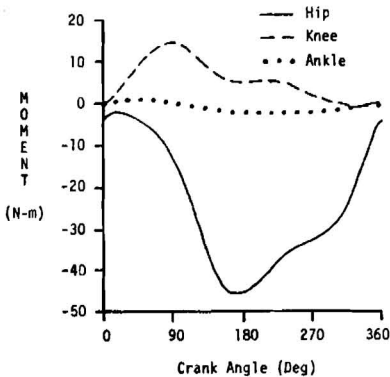


Fig. 5a Joint Moments Due to Acceleration (reference)

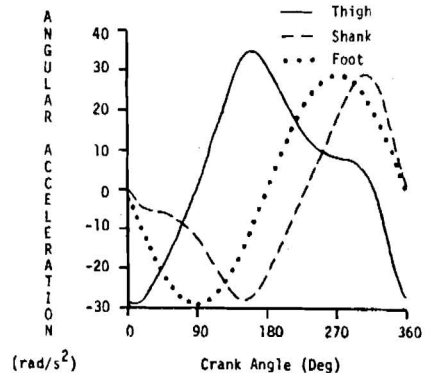


Fig. 5b Segment Angular Acceleration (reference)

The tibialis anterior becomes active at an inflexion point in the ankle flexion pattern at about 300° . The ankle moment, which corresponds to tibialis anterior activity, is close to zero and muscle activity bears little relationship to the pedal forces. Hence, the muscle flexes the ankle, thereby controlling the kinematics of the system.

In considering the hip joint, the inertia of the thigh is large and there is an intuitive dependence of the kinematic hip moment on angular acceleration. Figures 5(a) and 5(b) show that indeed the kinematic hip moment tracks the thigh angular acceleration. Maximum and minimum values occur at the same crank angle. Also, examination of Figures 4(a) and 5(a) shows that the inertial contribution to the total moment is significant.

Examination of the pedal load (Fig. 4(b)) and the quasi-static hip moment (Fig. 4(a)) shows that both the hip moment and normal pedal force increase in magnitude between TDC and 100° . Inasmuch as the tangential pedal force is nearly constant, it appears that the quasi-static hip moment is controlled primarily by the normal pedal force in this region. In the region 100° to 200° , however, the quasi-static hip moment continues to increase as the normal pedal force decreases. Examining the direction of the resultant pedal force vector sheds light on this peculiarity. As the crank arm travels through the region between 100° and 200° , the resultant of the normal and tangential pedal forces is in a direction such that the moment arm of the resultant increases. From 200° to TDC, the quasi-static hip moment and normal pedal force both decrease. Hence, in the regions TDC to 100° , and 200° to TDC, the quasi-static hip moment is influenced by the normal pedal force. Between 100° and 200° , the hip moment is controlled by a combination of the tangential and normal pedal forces.

Superimposing the quasi-static and kinematic hip moments leads to an interesting result. Note that the quasi-static moment is always positive and exhibits a maximum at about 170° , while the kinematic moment is always negative and exhibits a minimum at about 180° . When the two moments are added, the total hip moment (Fig. 6) is substantially lower than either of the two contributors. Observe also that the magnitude of the quasi-static moment is greater than the kinematic in the region 0° to 300° , while the reverse is true in the region 300° to 360° . This observation accounts for the polarity change at 300° in the total hip moment profile.

The muscles, which cross the hip joint, include the gluteus maximus, the biceps femoris, the semimembranosus, and the rectus femoris. The maximum activity region of the gluteus maximus is 20° to 100° , which corre-

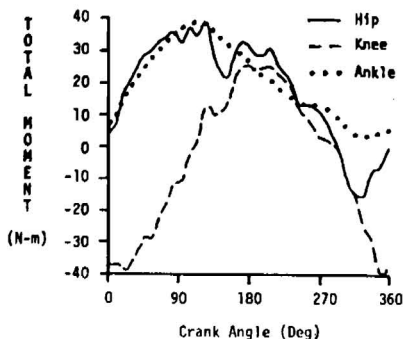


Fig. 6 Total Joint Moment (reference)

sponds to the increase in total hip moment. Because the quasi-static hip moment dominates the total moment in this region, it can be concluded that the gluteus maximus, aided by inertial characteristics, produces the normal pedal force. Both hamstring muscles exhibit greatest activity between 100° and 200°, where the total hip moment is sustained. Similar to the gluteus maximus, kinematics play a beneficial role in reducing the effort of the hamstrings. Rectus femoris activity correlates to the negative region of the total hip moment plot. Because the quasi-static hip moment approaches zero in this region, the rectus femoris plays a distinct role in the kinematics of pedalling.

Unlike the hip joint, it is difficult to relate the kinematic knee moment to the segment accelerations. This difficulty arises from relative motion and a lengthy discussion is not warranted. It is possible, however, to relate the quasi-static knee moment in Fig. 4a to the pedal forces in Fig. 4b. The primary observation is that the quasi-static knee moment is influenced mainly by the tangential pedal force and bears little relation to the normal pedal force.

An interesting conclusion results from examining the total knee moment (Fig. 6) in some detail. The kinematic knee moment is virtually always positive with a peak value of 15 Nm occurring at 90°. The quasi-static knee moment, on the other hand, shifts polarity with the negative peak of -40 Nm observed at 45° and a positive peak of 20 Nm observed at 180°.

TABLE 3. Percent difference of IEMG between Case 5 and the reference

region of max activity		17.3	53.8	81.2	131.4	167.9	204.4	240.9	277.4	313.9	350.4
27°-87°	GM	-31.2	-8.8	-36.4	-44.3	-6.6	222.0	139.2	66.5	55.7	-39.3
267°-29°	RF	35.1	15.7	51.4	-1.6	-15.4	45.3	60.1	105.6	-7.8	0.6
304°-90°	VM	-52.1	-28.2	-28.9	-16.3	37.7	-30.3	9.5	37.8	-6.2	-15.8
329°-90°	VL	-0.6	-40.1	-13.8	-88.2	-77.7	-52.4	-84.0	-87.4	-46.4	2.8
290°-3°	TA	-45.7	-78.0	-64.0	-39.7	-16.1	-8.4	-18.8	-32.8	-17.1	-14.6
84°-242°	G	-50.1	-43.8	-29.5	7.0	-21.3	-23.9	6.4	-34.6	-37.1	-22.5
100°-181°	BF	54.8	-36.9	-37.3	-13.3	-31.6	-46.5	69.3	-7.3	-22.9	-9.7
72°-192°	S	-54.3	-21.2	-5.2	-8.1	-20.9	-23.6	-36.8	-53.0	-31.7	-48.1

Table 4 Percent difference of IEMG between Case 6 and the reference

region of max activity		17.3	53.8	81.2	131.4	167.9	204.4	240.9	277.4	313.9	350.4
2°-110°	GM	-21.8	-13.9	-6.6	22.6	-11.9	276.6	158.6	0.7	-9.5	8.2
297°-45°	RF	79.0	192.7	94.2	32.6	-10.5	149.9	64.0	-4.5	59.9	59.3
302°-100°	VM	-20.2	-30.7	9.5	22.4	70.2	10.8	42.7	-1.7	45.5	9.3
307°-72°	VL	43.0	3.7	28.3	-85.4	-75.0	-30.2	-79.7	-79.0	55.5	64.8
302°-14°	TA	-25.1	-81.1	-65.9	-61.0	-30.0	-53.7	-18.6	23.8	8.6	28.0
54°-247°	G	-59.8	-25.3	-11.0	-13.4	-4.6	-2.8	1.2	18.3	-32.8	-48.5
96°-202°	BF	75.1	-32.4	2.2	-5.4	11.8	31.4	202.7	-6.4	-18.1	30.2
103°-220°	S	-36.8	7.7	2.4	1.1	19.3	58.4	38.5	-23.0	28.2	-20.9

Because the kinematic and quasi-static peak moments are not in phase, combining the two yields a total knee moment where neither magnitude nor shape varies markedly from the quasi-static moment. Accordingly, it appears that pedalling rate (i.e. cadence) has a more profound affect on the hip moment.

The muscle activity picture at the knee is complicated by the fact that all of the muscles monitored except for the tibialis anterior and the gluteus maximus cross the knee joint. In the discussion of the hip joint, it was noted that rectus femoris activity spans the region 300° to TDC. The 300° point corresponds to the zero crossing of the total knee moment which in turn corresponds to the onset of increasing tangential pedal force. Accordingly, the rectus femoris not only affects the motion of the leg, but also develops the tangential pedal load. The greatest activity of the vastii muscles occurs in the region 350° - 80° , which includes the maximum magnitude of the total knee moment. Note that the total knee moment is influenced primarily by the tangential pedal load in this region. Accordingly, the vastii muscles generate the knee moment which is necessary to sustain the tangential pedal force. Because the hamstrings are antagonistic to the quadriceps, they act to produce the positive total knee moment in the 100° to 200° region. Note that the positive total knee moment results from positive contributions of both the kinematic and quasi-static moments. Hence, the hamstring muscles contribute both to generating the pedal forces and driving the leg linkage.

B. Cases 5 and 6:

The effects of higher versus lower gear ratios are apparent in the pedal force profiles (Figs. 7a and 7b) and crank torque curves (Fig. 8a). The crank torque curves indicate that the peak torque, which occurs at 90° , is directly related to the gear ratio. Because the magnitude of the normal pedal force exhibits the same trend, the source of the torque increase is the normal pedal force rather than the tangential pedal force. The crank torque curves also indicate differences in the minimum torque with the negative torque region for Case 6 significantly less than for both Case 5 and the reference. The reduction of the negative torque region for Case 6 is due to the combined effects of changes in the tangential and normal pedal force profiles. Not only is the magnitude of the negative pedal force decreased, but also a significant negative tangential shear is developed. These results illustrate the profound effect that changes in the pedal force profiles have on the crank torque.

In the analysis of joint moments, one need only compare the moments due to pedal load because the pedalling rate is the same as the reference for Cases 5 and 6. In comparing the hip moment (Fig. 8b) for Cases 5 and 6 in the region between the TDC and 100° , the moment for Case 5 is consistently lower than Case 6. It was noted earlier that the gluteus maximus activity corresponded to the increase in hip moment from 0° to 100° . Accordingly, one expects lower gluteus maximus activity when Case 5 is compared with Case 6. This is indeed the case; there is about a 72 percent difference in muscle activity between Cases 5 and 6 when IEMG is compared (see Tables 3 and 4). Between 100° and 200° , the hamstrings are

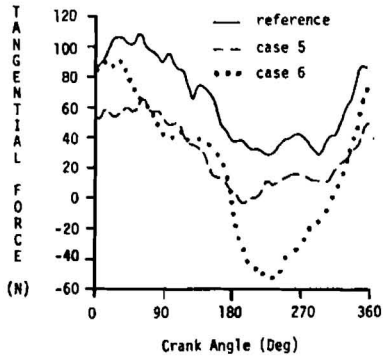


Fig. 7a Tangential Pedal Load (Cases 5 and 6)

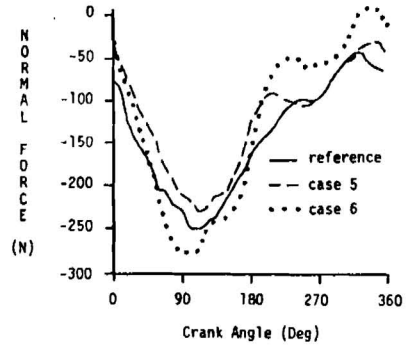


Fig. 7b Normal Pedal Load (Cases 5 and 6)

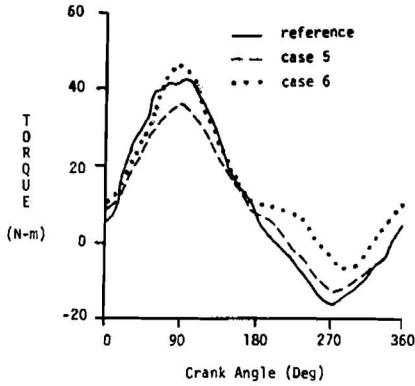


Fig. 8a Torque Curves (Cases 5 and 6)

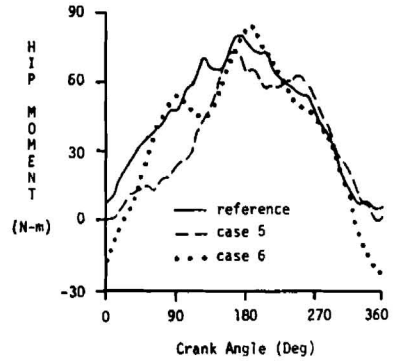


Fig. 8b Hip Moment Due to Pedal Load (Cases 5 and 6)

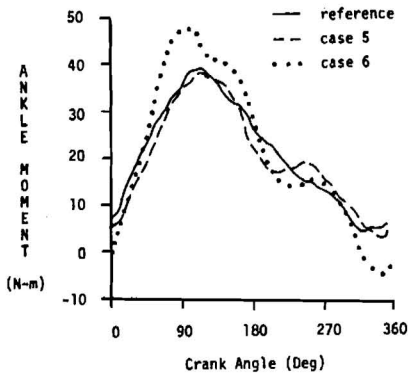


Fig. 9a Ankle Moment Due to Pedal Load (Cases 5 and 6)

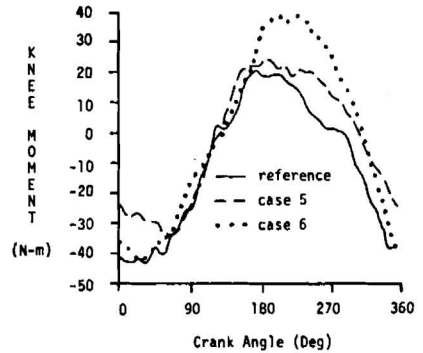


Fig. 9b Knee Moment Due to Pedal Load (Cases 5 and 6)

responsible for the hip moment. Case 6 and the reference exhibit both comparable moments and IEMG results. Case 5 is somewhat lower than the reference in both the moment plot and IEMG levels. Similar to the gluteus maximus, the hamstring activity may be predicted at least qualitatively from the moment plots. The activity of the rectus femoris exhibits no significant change for Case 5 compared to the reference. Case 6, however, indicates an average 65 percent increase in the maximum activity region. Note that the rectus femoris activity corresponds closely to the negative hip moment in the region 300° to 20° .

The analysis of the ankle joint leads to an anomalous result. Examination of Fig. 9a shows that the ankle moment for Case 5 and the reference track one another whereas Case 6 exhibits a significant increase between 40° and 180° . The increase in ankle moment is consistent with the increase in magnitude of the normal pedal force. One would expect that because the gastrocnemius equilibrates the ankle moment, gastroc activity for Case 6 would be greater than the reference and would exhibit little difference between Case 5 and the reference. Inspection of IEMG levels shows, however, that this is not the case. The gastroc IEMG level for Case 6 decreases an average of 8 percent between 80° and 200° . For Case 5, IEMG decreases an average of 15 percent for the same region. Inasmuch as other muscles (e.g. soleus), which are capable of supporting a positive ankle moment were not monitored, it appears that these muscles play redundant roles. In an earlier study by Jorge and Hull [19], the soleus was shown to have a supporting role to the gastrocnemius.

The negative excursion of the ankle moment for Case 6 just before TDC is reflected by the tibialis anterior, which shows an increase in activity. Examination of Case 5 shows no significant change here. This is expected because the ankle moments for Case 5 and the reference are similar.

The knee moment plot (Fig. 9b) shows two striking features. The first is in the region between TDC and 70° , where the magnitude of the knee moment for Case 5 is less than both Case 6 and the reference which are comparable. An earlier observation was that the vastii muscles sustain the negative knee moment; hence, a decrease in vastii activity would be expected. Case 6 exhibits an average of 5.7 percent increase for the vastii muscles which is not notable. For Case 5, there is an average of 27 percent decrease in vastii activity.

A second striking feature in the knee moment plot is the contrast in the positive knee moment in the region between 180° and 300° , where both Cases 5 and 6 are above the reference. This characteristic of the knee moment plot is expected because of the change in pedalling technique reflected in the minimum value of the tangential load. Accomplishing the negative tangential load in Case 6 would require an increase in hamstring activity when compared with the reference. This is indeed the case. There is an average increase of about 50 percent for the hamstrings in Case 6 when compared with the reference. An average decrease of 16 percent for hamstring activity is seen for Case 5, which is not a marked change.

Concluding Remarks

Although the discussion in the body of the paper is devoted to the data for test subject A, similar data was generated for subjects B and C. To examine the consistency of the conclusions drawn for test subject A, the data for subjects B and C were compared against that of subject A. For the reference case, it was observed that the characteristics (i.e. shape and phase) of the pedal force profiles, hence quasi-static moment plots, were similar. Due to different styles of pedalling, magnitudes of both peak loads and moments varied considerably, however. Kinematic moment plots were not only consistent in shape, but also in magnitude.

In comparing the data for subjects B and C to that of subject A for Cases 5 and 6, it was observed that the pedal loading and hence quasi-static moments exhibited similar trends. Subjects B and C showed improved correspondence between muscle activity levels and joint moments. The anomalous activity observed for subject A of the gastroc was not seen for subjects B and C. Subjects B and C appeared to have pedalled more consistently, which may explain the improved correlation.

In addition to Cases 5 and 6, which explored the biomechanics of pedalling under pedal load changes at constant cadence, Table 2 indicates that data were also recorded for Cases 3 and 4. Cases 3 and 4 were undertaken to explore the biomechanics of pedalling under changes of cadence with constant power output. Note that achieving constant power requires changing two variables (i.e. cadence and pedal load), both of which influence joint moments. Because of space limitations, a detailed discussion of Cases 3 and 4 is not included here. Such a discussion can be found, however, in Ref. [20]. The findings relevant to Cases 3 and 4 are summarized as follows:

- 1) Both normal and tangential pedal loads are inversely related to cadence.
- 2) The total hip moment is more strongly affected by cadence than the total knee moment. Peak moments of both the hip and the knee are inversely related to cadence within the range studied (63-97 RPM).
- 3) Muscle activity levels do not correlate well to joint moments. The lack of correlation may be due to the complexities of simultaneously varying two quantities, both of which affect joint moments.

With the above comments in mind, the hypotheses which guided this research can be evaluated. Cases 5 and 6 establish a strong dependence of joint moments on pedal loading so that the first hypothesis is valid. Cases 3 and 4 illustrate that kinematic moments at the hip and knee joints are significant at cadence above 60 RPM and are on the same order as quasi-static moments at 100 RPM. Accordingly, the second hypothesis appears valid. The muscle activity in Cases 5 and 6 validates the third hypothesis while the activity picture in Cases 3 and 4 is not conclusive. More conclusive results might be obtained from additional tests which vary kinematic moments while holding quasi-static moments constant.

Acknowledgement

The authors are grateful to the University of California Appropriate Technology Program (Grant No. 83-14-6000) for supporting this work.

References

1. Houtz, S. J. and Fischer, F. J., "An Analysis of Muscle Action and Joint Excursion on a Stationary Bicycle," The Journal of Bone and Joint Surgery, Vol. 41A, No. 1, pp. 123-131, Jan. 1959.
2. Despires, M., "An Electromyographic Study of Competitive Road Cycling Conditions Simulated on a Treadmill," Biomechanics IV, University Park Press, Baltimore, MD, pp. 349-355, 1974.
3. Faria, I. E. and Cavanagh, P. R., The Physiology and Biomechanics of Cycling, John Wiley and Sons, Inc., New York, 1978.
4. Gregor, R. J., Green, D., and Garhammer, J. J., "An Electromyographic Analysis of Selected Muscle Activity in Elite Competitive Cyclists," Biomechanics VII, University Park Press, Baltimore, MD, pp. 537-541, 1982.
5. Jorge, M. and Hull, M. L., "Analysis of EMG Measurements During Bicycle Pedalling," submitted to the Journal of Biomechanics, July 1983.
6. Goto, S., Toyoshima, S., and Hoshikawa, T., "Study of the Integrated EMG of Leg Muscles During Pedalling of Various Loads, Frequency, and Equivalent Power," Biomechanics V-1A, University Park Press, Baltimore, MD, Vol. 1A, pp. 246-252, 1976.
7. Hoes, J. J. A. J. M., Binkhorst, R. A., Smeekes-Kuyt, A. E. M. C., Vissers, A. C. A., "Measurement of Forces Exerted on Pedal and Crank During Work on a Bicycle Ergometer at Different Loads," Int. Z. Angew. Physiol. Einschl. Arbeitsphysiol., Vol. 26, pp. 33-42, 1968.
8. Gregor, R. J., A Biomechanical Analysis of Lower Limb Action During Cycling at Four Different Loads, University Microfilms International, Ann Arbor, MI, 1976.
9. Hull, M. L. and Davis, R. R., "Measurement of Pedal Loading During Bicycling - I. Instrumentation," Journal of Biomechanics, Vol. 14, No. 12, pp. 843-855, 1981.
10. Nordeen-Snyder, K. S., "The Effect of Bicycle Seat Height Variation Upon Oxygen Consumption and Lower Limb Kinematics," Medicine and Science in Sports, Vol. 9, No. 2, pp. 113-117, 1977.
11. Winter, D. A. and Robertson, D. G. E., "Joint Torque and Energy Patterns in Normal Gait," Biological Cybernetics, Vol. 29, pp. 137-142, 1978.

References (continued)

12. Zarrugh, M. Y., "Kinematic Prediction of Intersegment Loads and Power at the Joints of the Leg in Walking," Journal of Biomechanics, Vol. 14, No. 10, pp. 713-725, 1981, Pergamon Press, Great Britain.
13. Andrews, J. G., "On the Relationship Between Resultant Joint Torques at the Joints of the Leg in Walking," Medicine and Science in Sports and Exercise, Vol. 14, No. 5, pp. 361-367, 1982.
14. Chao, E. Y. and Rim, K., "Application of Optimization Principles in Determining the Applied Moments in Human Leg Joints During Gait," Journal of Biomechanics, 1973, Vol. 6, pp. 497-510, Pergamon Press, Great Britain.
15. Ghista, D. N., Toridis, T. G. and Srinivasan, T. M., "Human Gait Analysis: Determination of Instantaneous Joint Reactive Forces, Muscle Forces, and the Stress Distribution in Bone Segments - Part II," Biomedizinische Technik, Vol. 21, pp. 66-74.
16. Seireg, A. and Arvikar, R. J., "A Mathematical Model for Evaluation of Forces in Lower Extremities of the Musculo-Skeletal System," Journal of Biomechanics, 1973, Vol. 6, pp. 313-326, Pergamon Press, Great Britain.
17. Davis, R. R. and Hull, M. L., "Measurement of Pedal Loading During Bicycling - II. Analysis and Results," Journal of Biomechanics, Vol. 14, No. 12, pp. 857-872, 1981.
18. Drillis, R. and Contini, R., Body Segment Parameters, New York University, N.Y., Technical Report No. 1166.03, 1966.
19. Jorge, M. and Hull, M. L., "Preliminary Results of EMG Measurements During Bicycle Pedalling," 1983 Biomechanics Symposium, ASME, AMD, Vol. 56, pp. 27-30.
20. Jorge, M. and Hull, M. L., "Biomechanics of Bicycle Pedalling," submitted to the Journal of Biomechanics.